Disturbance Effects Of Animal Carcass Decomposition On Microbial Communities And Virulence Genes In River Water

Xiaojing Wang

Zhoukou Vocational and Technical College, Zhoukou 466000, China

Corresponding author. E-mail: wxj900709@163.com

Received: Nov. 28, 2025; Accepted: Feb. 10, 2026

Under the influence of climate change and human activities, the retention of animal carcasses in river water has become increasingly frequent, posing disturbances to the physicochemical properties and ecosystem of river environments. This study analyzes the impact of carcass decomposition on river ecosystems by measuring changes in water physicochemical parameters, microbial community structure, and the abundance of virulence genes. The results show that decomposition significantly decreases Dissolved Oxygen levels in water, with the lowest concentration reaching 0.08 mg/L. Meanwhile, ammonium nitrogen concentration rises sharply to 14.32 μg/ml, whereas nitrate nitrogen shows minimal change. Among microbial groups, bacteria are the dominant group, with a relative abundance of >60%. However, the abundance of archaea increases significantly in the carcass group ($p<0.05$). Analysis of virulence genes indicates that genes such as phoP and glnAl reach their highest abundance at 32°C in the carcass group. The structure of virulence gene profiles is strongly correlated with microbial communities, as shown by Procrustes analysis ($r=0.810$, $p<0.05$). These findings demonstrate that carcass decomposition drives microbial succession and promotes the enrichment of virulence genes by altering oxygen availability and nitrogen cycling. This provides valuable data for understanding the link between organic pollution and pathogenic risk in river ecosystems.

Keywords: River water; Animal carcass decomposition; Microbial communities; Virulence genes; Disturbance effects

http://dx.doi.org/10.6180/jase.202609_32.030

1. Introduction

Animal carcass decomposition in river water plays an important role in the material cycling of natural ecosystems. However, the release of organic matter and metabolic byproducts such as biogenic amines and hydrogen sulfide may disrupt the physicochemical balance of the water, leading to changes in microbial community structure and activation of virulence gene expression [1]. Specifically, during the decomposition of corpses, a large amount of organic matter and metabolic byproducts such as biogenic amines and hydrogen sulfide are released. These compounds disrupt the physicochemical balance of water through various mechanisms. Biogenic amines can serve as nitrogen sources and alter local pH , while hydrogen sulfide has cytotoxicity and can inhibit aerobic microorganisms, creating a strong reducing microenvironment. This imbalance not only directly leads to the replacement of microbial community structure, but may also regulate the horizontal transfer or expression activation of virulence genes by activating microbial quorum sensing systems, oxidative stress response pathways, and transmembrane transporter protein expression, ultimately potentially increasing the risk of disease in water bodies.

Microorganisms play a complex and dynamic dual role in natural ecosystems. In a healthy host or stable environment, it often colonizes as a normal microbial community, inhibiting the invasion of foreign pathogens and maintain-

ing the healthy balance of the host or ecosystem by occupying ecological niches, competing for nutrients, and producing antibacterial substances. For example, in mammalian liver, specific resident microbial communities are believed to be involved in the metabolism of primary bile acids and immune regulation. However, this symbiotic relationship is fragile. When environmental conditions undergo drastic changes, such as hypoxia, pH changes, overnutrition, or the presence of a large amount of necrotic tissue, the original microecological balance will be disrupted. Some originally harmless normal bacterial populations or conditionally pathogenic bacteria may proliferate and transform into actual pathogenic bacteria by expressing virulence genes they carry, such as genes encoding adhesins, invasions, or toxins, or by obtaining new virulence factors through horizontal gene transfer. Therefore, the potential pathogenic risk of microbial communities is not fixed and unchanging, but deeply rooted in the environmental context in which they exist. Current studies show that carcass decomposition can cause depletion of Dissolved Oxygen (DO) and accumulation of ammonium nitrogen. These environmental stresses may promote the proliferation of pathogenic bacteria and horizontal transfer of virulence genes. However, systematic research on the combined effects of physicochemical parameters, microbial communities, and virulence genes is still lacking [2, 3]. For example, the team led by Barceló finds that decomposition reshapes trophic cascade features in communities but does not explore the response of virulence genes [4]. Although Rasmi's group examines the distribution of virulence genes, they do not consider the dynamic changes in environmental factors [5]. $NO_3 - N$ is a major form of nitrogen in water and significantly affects both DO and pH levels.

The UV spectrophotometric method for $NO_3 - N$ is based on the specific absorption of nitrate ions in the ultraviolet range. Absorbance at 275 nm is used to correct for organic matter interference. This study addresses the gap by simulating animal carcass decomposition in river water under different temperatures. It monitors the variation in water DO, ammonium nitrogen concentration, microbial community α - and β-diversity, and virulence gene abundance. The goal is to investigate how animal carcass decomposition disturbs river ecosystems in the context of global warming. By integrating high-throughput metagenomic analysis in bioinformatics with a heatmap of virulence genes, this study innovatively analyzes the linkage between microbial communities and virulence genes. It not only fills the knowledge gap in understanding how carcass decomposition affects microbial virulence potential but also offers theoretical support for evaluating ecological risks of organic pollution and developing control strategies.

2. Materials and methods

2.1. Preparation Design of River Water Samples with Decomposing Animal Carcasses

2.1.1. Experimental materials and instruments

Animal carcasses in river water act as complex organic matter carriers. Their decomposition not only disrupts the balance of carbon and nitrogen cycling in water, but also releases metabolic byproducts such as biogenic amines and hydrogen sulfide. These compounds may induce microbial community succession and trigger the horizontal transfer or expression regulation of virulence genes [6, 7]. To investigate the disturbance effects of carcass decomposition on microbial communities and virulence genes in river water, this study first designs an experiment to prepare water samples containing decomposing animal carcasses. The study employed artificial simulation to prepare river water samples containing decomposed animal carcasses, rather than directly collecting samples from natural pollution areas. This approach aimed to control environmental variables, enhance experimental reproducibility, reduce biosafety risks, and facilitate a systematic exploration of the direct impact mechanisms of temperature and carcass decomposition on microbial communities and virulence genes. This provides a theoretical basis for subsequent related research in natural water bodies. The required instruments for preparing samples with decomposing animal carcasses are listed in Table 1.

In Table 1, 30-liter plastic buckets are used to collect river water on site to ensure sample representativeness. A WQG-11 water thermometer monitors water temperature in real time. A 40-liter constant temperature water bath serves as the main reaction vessel simulating natural thermal conditions. A CN-010 sterile submersible heater provides temperature control while preventing external contamination, and is suitable for sealed reaction settings. Sampling sites are selected to avoid any pollution discharge outlets within 500 meters upstream or downstream. No rainfall should occur during the week prior to sampling, and surface river water is chosen. Personnel wear sterile disposable gloves during sampling, and the collected water is immediately sealed. Water quality parameters are measured using a UV-visible spectrophotometer. Microbial cells in the water are retained using microporous membranes, which also filter out large particles.

2.1.2. Design of experimental procedures

Based on the functional characteristics of the instruments and standardized water sampling, the experiment is then

Table 1. Instruments used for preparing samples with decomposing animal carcasses

Material	Specification	Manufacturer
Electronic Balance	JD3000-2	LONGTECH
Square Constant-Temperature Water Tank	40 L	YIHENG
Volumetric Flask	1000 mL	TIANBO
Aqueous Microporous Filter Membrane	50 mm × 0.22μ m, 50 mm × 5μ m	JINTENG
Beaker	200 mL, 1000 mL	SHUNIU
Plastic Sampling Bucket	30L	HUANYU
Water Thermometer	WQG-11	DEQIAN
Underwater Aseptic Heating Rod	CN-010	BAISHI
Pipette	Research plus	Eppendorf
UV Transilluminator	GL-3120	QILINBELL
UV-Vis Spectrophotometer	NANO DROP One	THERMO

designed to simulate the decomposition process of animal carcasses. It includes procedures for sample handling, control group design, and environmental condition settings. The preparation process of water samples is shown in Fig. 1.

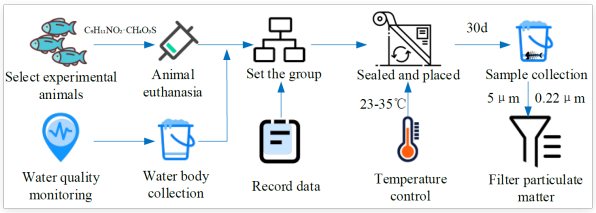

Fig. 1. Flow chart of water sample preparation with decomposing animal carcasses

As shown in Fig. 1, the study first selects experimental animals and base water samples. All animals are euthanized using $C_9H_{11}NO_2 \cdot CH_4O_3$ S to avoid variability. Water is collected from upstream surface sources that meet the requirements of no pollution discharge outlets and no rainfall interference. The 40-liter water baths are completely sealed. Sterile submersible heaters are used for temperature control, simulating the global average temperature. After 30 days, 5μ m microporous membranes are used to remove large particles, followed by 0.22μ m membranes to capture microbial cells in the water. These filtered samples are used to analyze microbial community structure and virulence gene disturbance. Groups with added carcasses are defined as the carcass group, while those without are defined as the control group. Environmental parameters for each group are shown in Table 2.

Table 2 shows that the water volume is set at 40 liters. Animal carcasses and water temperature are selected as core variables. Five temperature levels are set at 23°C, 26°C, 29°C, 32°C, and 35°C, all suitable for microbial growth. The environmental parameter configurations for different experimental groups were repeated five times for each experiment. To minimize the influence of carcass weight on the results, the weight of carcasses is controlled at 106.40 ± 2.28 g. After grouping, each tank is sealed with sterile transparent film. After 30 days, the tanks are opened and filtered again to obtain the final water samples, which are used for microbial community and virulence gene analysis.

2.1.3. Measurement design for physicochemical properties of water samples

To clarify the physicochemical characteristics of water during carcass decomposition, the study conducts quantitative tests of each group's water samples after the experiment. Conductivity (CON), Total Dissolved Solids (TDS), Salinity, pH, and Oxidation-Reduction Potential (ORP) are measured using a benchtop water quality analyzer. Nitrate-Nitrogen ($NO_3 - N$) is measured by ultraviolet spectrophotometry, and Ammonia Nitrogen ($NH_4 - N$) is determined using the Nessler's reagent spectrophotometric method[8, 9]. The calculation of the corrected absorbance is shown in Equation (1) [10, 11].

$$A_{\text{Correction}} = A_{220} - 2 \times A_{275} \tag{1}$$

In Equation (1), A_{220} represents the absorbance at 220 nm, A_{275} represents the absorbance at 275 nm , and $A_{\text{Correction}}$ is the corrected absorbance value. Free NH_3 ions are lipid-soluble molecules that can penetrate biological membranes, damage fish gill tissues and nervous systems, and exhibit strong toxicity. The Nessler's reagent method forms a yellow-brown complex after the reaction between ammonia and the reagent, which is then used to determine the concentration of $NH_4 - N$ in the water. The calculation formula is shown in Equation (2).

$$C = \frac{A - b}{k} \times \frac{V}{V_{\text{Sampling}}} \tag{2}$$

Table 2. Environmental parameter configurations for different experimental groups

/			Add the weight of the corpse (g)			
Temperature (°C)	Volume of water (L)	Control group	Corpse Group 1	Corpse Group 2	Corpse Group 3	Corpse Group 4
23	40	0	105.23	106.89	104.56	107.31
26	40	0	106.12	108.05	104.98	107.54
29	40	0	105.78	107.92	104.15	108.60
32	40	0	106.95	105.30	107.81	104.42
35	40	0	104.87	108.33	105.64	107.19

In Equation (2), A represents the measured absorbance of the solution, k is the slope of the fitted linear equation, and b is the intercept.

2.2. Analysis of Disturbance Effects on Microbial Communities and Virulence Genes

2.2.1. *Experimental materials and instruments*

Water physicochemical characteristics of decomposing animal carcass samples in river water reflect to some extent the degree of water quality deterioration and nutrient enrichment. However, these indicators alone cannot directly reveal the disturbance effects of carcass decomposition on microbial communities and virulence genes. It is necessary to extract and classify microbial DNA from the samples and analyze them using biostatistical and bioinformatic approaches [12, 13]. The instruments required for microbial communities and virulence genes are listed in Table 3.

As shown in Table 3, a TissueLyser II bead mill is used to lyse microbial cells efficiently through physical disruption. An Eppendorf 5425 centrifuge completes the nucleic acid separation process. The DYY-8C electrophoresis system enables agarose gel electrophoresis to assess the integrity of extracted DNA. The C1000 Thermal Cycler and Veriti Thermal Cycler provide gradient PCR conditions for optimizing amplification of virulence gene-specific primers. The QuantStudio 3 real-time PCR system quantifies the copy number of virulence genes. Illumina NextSeq 550 and NovaSeq 6000 platforms support full-length 16S rRNA and metagenomic sequencing, providing data for community structure analysis and virulence gene cluster screening. Reagents and suppliers used in this analysis are summarized in Table 4.

As shown in Table 4, the TaKaRa DNA Gel Extraction Kit is used for secondary purification of PCR products to ensure sequence integrity. Agarose and nucleic acid stains are used with the DYY-8C system for visualizing nucleic acid fragments. Glacial acetic acid and sodium hydroxide are used to prepare Tris-acetate (TAE) buffer for stabilizing pH during electrophoresis. The Trans2K® DNA Marker, in combination with the TaKaRa TB Green ™ Premix Ex Taq ™ II real-time PCR system, is used to calibrate the molecular weight of amplification products. Ethylenediaminetetraacetic Acid (EDTA) serves as a chelating agent in solution preparation.

2.2.2. *Detection methods for microbial communities and functional genes in samples*

In this analysis of microbial communities and virulence genes, confirming the required instruments and reagents is essential for subsequent experiments. Based on these conditions, the study focuses on the design of detection methods for microbial communities and functional genes. High-purity microbial DNA extraction requires repeated centrifugation steps. The extraction process is shown in Fig. 2.

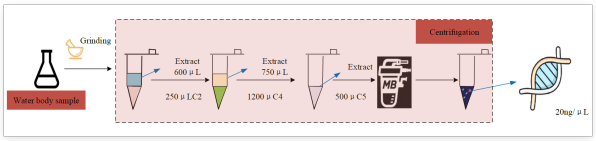

Fig. 2. Extraction process of high-purity microbial DNA from samples

As shown in Fig. 2, microbial DNA extraction involves multiple centrifugation steps. First, the fragmented filter membranes are mixed with Solution C1 for initial lysis and solid-liquid separation. The supernatant is collected. Second, the supernatant is mixed with LC2 and centrifuged at 10,000 g for 1 min at 4°C to remove protein impurities. Third, Solution C3 is added, and the mixture is centrifuged at the same speed for 1 min . Fourth, the supernatant is mixed with C 4 and centrifuged again. Finally, the eluate is filtered through a spin column and centrifuged for 30 s to obtain high-purity microbial DNA at a concentration of 20ng/μL.

Table 3. Summary of instruments for analyzing disturbance effects on microbial communities and virulence genes

Material	Specification	Manufacturer
Sequencer	Illumina Nextseq 550, Illumina Novaseq 6000	Illumina
Electrophoresis Apparatus	DYY-8C Type	BJ LY
PCR Amplifier	C1000 Thermal Cycler	Bio-RAD
PCR Machine	Veriti Thermal Cycler	Applied Biosystems
Real-time Quantitative PCR	QuantStudio 3 QPCR SYSTEM	Thermo Fisher Scientific
Recirculating Water Multi-purpose Vacuum Pump	SHB-B95	ZZGW
Rotating Mixer	Vortex 3	IKA
High - Pressure Steam Sterilizer	LDZX-50KBS	SHENAN
Constant - Temperature Water Bath	HH-S24	JINGHONG
Centrifuge	Eppendorf 5425	Eppendorf
DO Meter	JPB-607A	XINRUI
Benchtop Water Quality Analyzer	DR1900	HACH
Aseptic Centrifuge Tube	5mL, 2mL	CORNING
Microwave Oven	M1-L213C	MIDEA
Bead Mill Homogenizer	TissueLyser II	QIAGEN

Table 4. Summary of reagent kits for analyzing disturbance effects on microbial

Experimental Reagent Name	Manufacturer
2× TSINGKE MASTER MIX (blue)	Novoprotein
3-Ethoxyacetyl aniline methanesulfonate	Macklin
Glacial Acetic Acid (Analytical Reagent Grade)	Sinopharm
DNeasy® PowerSoil® Kit	Thermo Fisher
DNA Gel Extraction Kit	TaKaRa
EDTA, Analytical Reagent Grade	Sigma-Aldrich
Gel Stain	Novoprotein
Sodium Hydroxide (Analytical Reagent Grade)	Kermel
Agarose	Sangon
Trans2K® DNA Marker	Yuheng
TaKaRa TB Green ™ Premix Ex Taq ™ II	Hongxun
Tris, Analytical Reagent Grade	Aladdin

2.2.3. Statistical analysis methods for disturbance assessment

Microbial DNA carries rich information on community composition and functional potential. Due to its complexity, traditional methods cannot efficiently interpret the data. Bioinformatic statistical methods allow accurate analysis of microbial communities and virulence genes[14]. The study uses DIAMOND v0.7.12 software, a high-throughput sequence alignment tool, to quickly obtain sequence similarity information. The sequences are interpreted across bacteria, eukaryotes, archaea, and viruses, and compared with virulence genes using the Pathogen Host Interactions (PHI-base) database. DIAMOND v0.7.12 uses sequence similarity algorithms and hash-based data structures to identify matching regions and speed up the alignment process. The formula for mapping short sequence fragments into hash values is shown in Equation (3).

$$\text{Hash}(S) = c_0 \times r^{k-1} + c_1 \times r^{k-2} + \ldots + c_{k-1} \quad (3)$$

In Equation (3), r represents the type of nucleotide base, and s represents a short sequence fragment of the gene. Microbial abundance in the carcass and control groups is visualized using custom heatmaps. The disturbance effects of carcass decomposition on microbial communities and virulence genes are evaluated by calculating microbial community β-diversity and applying statistical error correction to control false discovery rates. The Bray-Curtis (BC) index is used to measure species composition differences between ecological communities, and its calculation

is shown in Equation (4).

$$BC(i,j) = 1 - \frac{2 \times \sum_{k=1}^{S} \min(x_{ik}, x_{jk})}{\sum_{k=1}^{S} x_{ik} + \sum_{k=1}^{S} x_{jk}} \quad (4)$$

In Equation (4), xik and xjk represent the abundance of species k, and S is the total number of species. Community difference tests are performed using the vegan package.

3. Results and discussion

3.1. Verification of Changes in Physicochemical Parameters, Microbial Communities, and Virulence Gene Abundance

To explore the disturbance effects of animal carcass decomposition in river water on microbial communities and virulence gene abundance, the study tested the physicochemical parameters, microbial composition, and virulence gene profiles of the samples. Each group conducted five replicate experiments and took the average as the final result. Detailed physicochemical indicators of the water samples are shown in Table 5.

As shown in Table 5, the DO values in the carcass group were significantly lower than those in the control group, with the lowest value reaching 0.08mg/L, far below the 6.30mg/L observed in the control group. This indicated that the decomposition process consumed a large amount of oxygen. The NH_4-N concentration increased significantly from 0.22μ g/ml in the control group to 14.30μ g/ml in the carcass group, suggesting substantial NH_4-N release during decomposition. In contrast, the NO_3-N concentration showed only minor changes. The pH and TDS values remained relatively stable across groups, with the highest pH of 8.23 recorded in control group 4 , slightly higher than 7.75 in carcass group 1. These results indicated that animal carcass decomposition in river water consumed oxygen and released NH_4-N, potentially harming aquatic organisms. And these drastic physical and chemical changes may trigger a series of downstream ecological consequences. Firstly, sustained hypoxia stress can directly threaten the survival of fish and other aerobic aquatic organisms, leading to avoidance behavior, growth inhibition, and even death. Secondly, this oxygen deficient and ammonium rich environment creates strong selection pressure, which is conducive to promoting the proliferation of anaerobic microorganisms such as methanogenic archaea and ammonium/ammonia tolerant microbial communities, fundamentally altering the functional pattern of aquatic microbial ecosystems. Although the concentration of ammonium nitrogen increased sharply, the concentration of nitrate nitrogen changed very little throughout the entire experimental period. This is likely related to the inhibition of the dynamic equilibrium of nitrification denitrification under low dissolved oxygen conditions. Nitrification is mainly driven by aerobic microorganisms, and its rate significantly decreases in hypoxic environments; Denitrification is also limited by electron acceptors and specific anaerobic conditions. Therefore, in the strongly reducing microenvironment dominated by corpse decomposition, nitrogen cycling may be "locked" in the ammonium nitrogen stage or through other anaerobic nitrogen conversion pathways, thereby limiting the net accumulation of nitrate. To evaluate the effects of reduced DO and increased NH_4-N on microbial communities, the study analyzed the relative abundance of microbial groups
in the control and carcass groups. The results are shown in Fig. 3.

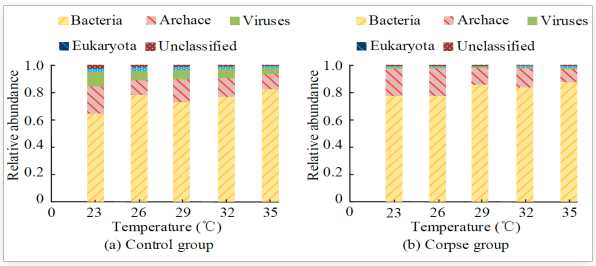

Fig. 3. Relative abundance of microbial communities in control and carcass groups

As shown in Fig. 3(a), the microbial community in the water included bacteria, archaea, viruses, eukaryotes, and unclassified groups. Bacteria dominated both groups at all temperatures, with relative abundance exceeding 0.6, and their proportion remained stable as temperature increased from 23°C to 35°C. Archaea ranked second in abundance, with an average relative abundance over 0.2 in the carcass group. Fig. 3(b) showed that the relative abundance of viruses, eukaryotes, and unclassified groups remained below 0.1 . Among the differences, the most significant increase was observed in the proportion of archaea in the carcass group. The PERMANOVA analysis based on Bray-Curtis distance indicated that temperature increase had a significant impact on the overall microbial community composition ($p < 0.05$). These findings suggested that changes in DO and NH_4-N altered the microbial community structure, with a significant rise in the relative abundance of archaea ($p < 0.05$). This growth is mainly attributed to the relative enrichment of anaerobic methane producing bacteria, such as Methanobacteria, and ammonia oxidizing archaea, such as the phylum Archaea. This indicates that in the hypoxic microenvironment caused

Table 5. Summary of physicochemical parameters in decomposing animal carcass samples

CON	TDS	Salinity	pH	ORP	DO	NH_4-N μg/ml	NO_3-N μg/ml
DZ1	785	0.40	8.05	-65.2	6.30	0.31	3.82
DZ2	910	0.45	7.95	-57.5	5.40	0.25	3.83
DZ3	880	0.44	8.15	-68.5	5.84	0.44	3.25
DZ4	870	0.45	8.20	-70.1	5.92	0.22	3.85
ST1	835	0.42	7.75	-14.2	0.08	13.50	0.55
ST2	710	0.35	7.64	-11.7	0.35	14.16	0.35
ST3	830	0.42	7.85	-22.0	1.60	14.30	0.43
ST4	740	0.38	8.23	-48.0	0.65	14.11	0.86

by corpse decomposition, strictly anaerobic methanogenic bacteria may proliferate by utilizing the hydrogen and carbon dioxide produced from decomposition for methane production, marking a shift from carbon cycling to anaerobic metabolic pathways. At the same time, the increase of archaea is directly related to the high concentration of ammonium nitrogen in the water. They participate in the nitrogen cycle by oxidizing ammonia to nitrite, which may partially alleviate the toxicity of high ammonia nitrogen to aquatic organisms, and also change the transformation path and destination of nitrogen elements in the water.

To assess the disturbance effects on virulence gene abundance, the study constructed a heatmap of the top 15 most abundant virulence genes in the water samples, as shown in Figure 4. The heatmap emphasizes the distribution of gene abundance states along the temperature gradient, displaying the relative abundance of the top 15 virulence genes in each group at different temperatures. The relative abundance of each virulence gene is calculated by normalizing its sequencing reads to the total number of highquality sequencing reads obtained from the corresponding sample, enabling crosssample comparison.

As shown in Fig. 4, the heatmap displayed the relative abundance of the top 15 virulence genes in the control and carcass groups across different temperatures. Warm colors represented high abundance, while cool colors indicated low abundance. The results showed that most virulence

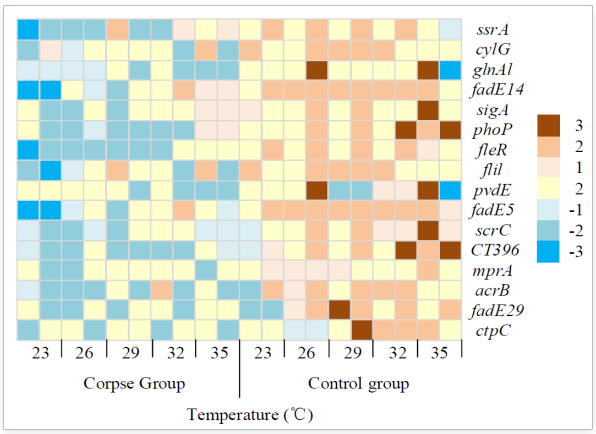

Fig. 4. heatmap of the top 15 virulence genes in water samples

genes had significantly higher abundance in the carcass group than in the control group. Genes such as phoP, glnAl, sigA, and CT396 peaked in the carcass group at 32°C. PERMANOVA analysis based on Bray Curtis distance confirmed a highly significant difference ($p < 0.01$) in the overall virulence gene profile between the control group and the cadaver group. The enrichment of these genes has important biological significance, among which phoP is a key component of the two-component regulatory system *PhoP/PhoQ*, widely involved in bacterial stress response

to low magnesium, acidic environments, and antimicrobial peptides, and regulating the expression of various virulence factors. GlnAl encodes glutamine synthetase, which is a core enzyme in microbial nitrogen metabolism. Its abundance changes are directly related to the metabolic pressure and nitrogen assimilation process of high concentrations of ammonium nitrogen in water. Sig A is the main sigma factor in bacteria, responsible for the transcription of housekeeping genes. Its expression level is often regarded as an indicator of microbial cells' ability to maintain basic vitality and metabolic recombination in response to environmental stress, such as hypoxia and nutrient limitation. Therefore, the peak of these genes at specific temperatures not only indicates an increase in virulence potential, but also reflects the profound physiological adjustments that occur in the microbial community to adapt to the hypoxic, nitrogen rich, and chemical stress microenvironment caused by corpse decomposition, including stress response, nitrogen metabolism recombination, and global transcriptional regulation. However, the abundance of certain siderophore synthesis genes first increased and then decreased with rising temperature. These findings indicated that carcass decomposition altered the water environment and significantly increased virulence gene abundance, raising the risk of environmental pollution.

3.2. Integrated Analysis of Dissimilarity and Diversity in Microbial and Virulence Gene Profiles

After confirming the disturbance effects of physicochemical changes on microbial communities and virulence genes, the study further focused on differences in community composition and diversity to explore the multidimensional impacts of carcass decomposition. Fig. 5 shows the heterogeneity of the GA gene community and the adjusted stochastic ratio in the control and carcass groups.

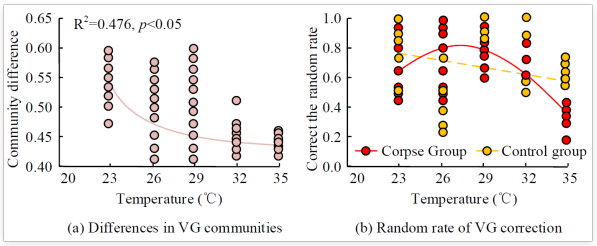

Fig. 5. Community dissimilarity and adjusted stochastic ratio of GA genes in decomposing river water samples

As shown in Fig. 5(a), the regression analysis results based on the Bray-Curtis distance matrix indicate that temperature has an explanatory power of $R^2 = 0.476$ ($p < 0.05$) for the differences in virulence gene profiles among cadaver groups. As temperature increases, this difference first decreases and then increases, reaching a minimum value of 0.46 at 32°C, which is significantly lower than the value of 0.56 at 23°C, and then tends to stabilize. In Fig. 5(b), red dots represented the carcass group and yellow dots represented the control group, showing the adjusted stochastic ratio. The ratio in the carcass group first increased to 0.83 and then declined to 0.38 at 35°C, while the control group remained dominated by randomness with no significant trend. The aforementioned results may be attributed to the fact that at moderate temperatures (such as $28 - 32$°C), the abundant organic matter provided by cadaver decomposition and the anaerobic environment may create a strong selective pressure, enabling the dominant amplification of a small number of microbial groups that are adapted to these conditions and carry specific virulence genes. This leads to reduced variability and enhanced deterministic selection within the entire virulence gene community. When the temperature continues to rise to 35°C, excessive thermal stress may inhibit the activity of some microorganisms while simultaneously triggering new and diverse stress response mechanisms, thereby increasing community variability once again and weakening the deterministic role of environmental filtration. This indicates that environmental perturbations from cadaver decomposition reshape the community structure of virulence genes, driving the assembly process from random diffusion to environmental filtration dominated by key factors such as temperature within a specific temperature range, such as around 28°C. The study also analyzed α and β diversity of virulence genes, as shown in Fig. 6.

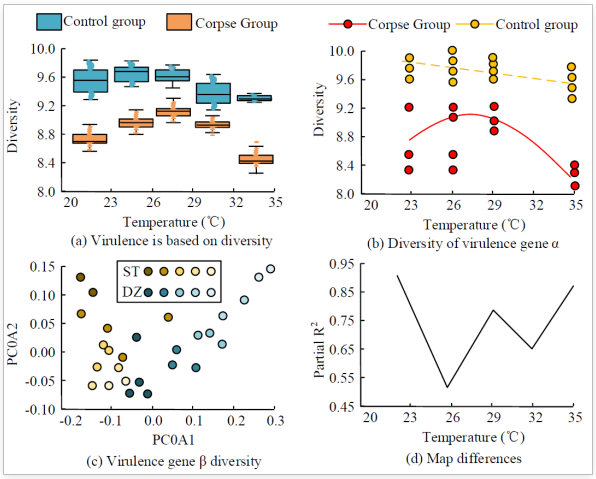

Fig. 6. Community diversity and ordination of virulence genes

As shown inFig. 6(a), with rising temperature, the α diversity of virulence genes in the control group remained higher than that in the carcass group. The median value in the carcass group decreased from 9.0 to 8.5, while the control group maintained a stable level of 9.5. Fig. 6(b) showed a continuous decline in α diversity in the carcass group, while the control group displayed little fluctuation, suggesting that decomposition amplified the suppressive effect of temperature on virulence gene richness. In Fig. 6(c), the clustering of gene communities was distinct. Carcass group samples were clustered around -0.1 , while the control group displayed a broader fluctuation over 0.3. In Fig. 6(d), the explanatory power of temperature on virulence gene community composition reached its lowest point at $26°C(0.45)$ and rebounded to 0.75 at 35°C, forming a U-shaped pattern. This indicated that factors beyond temperature also influenced gene community variation. These results showed that animal carcass decomposition reshaped the diversity pattern and assembly mechanisms of virulence genes by altering the microenvironment, providing insight into the adaptive evolution of their pathogenic potential. When the adjusted randomness ratio is significantly higher than 0.5 , it is generally believed that deterministic processes, such as environmental filtering, play a dominant role in community assembly. Research data shows that this ratio peaks at 0.82 at 28°C, and at this temperature, temperature acts as a key environmental filter, exerting the strongest deterministic selection pressure on the assembly of virulence gene profiles, driving the assembly process to shift from random diffusion to environmental filtering. The biological significance of this peak at 28°C may lie in its proximity to the optimal growth temperature range $(25-37°C)$ for many common gut and environmental bacteria. At this temperature, microorganisms from animal corpses exhibit high metabolic activity, and the large amount of organic matter released during decomposition and the resulting hypoxic environment together constitute a strong selection pressure, thereby effectively selecting and enriching microbial groups that carry specific virulence genes and are adapted to this microenvironment, resulting in the highest deterministic selection signal, i.e., the peak of the randomness ratio. When the temperature deviates from this range, the overall activity or stress response mechanisms of microorganisms change, and the intensity of environmental filtering also decreases accordingly. Finally, the study examined the alignment between microbial community structure and the distribution of GA genes using Procrustes analysis, as shown in Fig. 7.

As shown in Fig. 7, the figure visualizes Principal Coordinate Analysis (PCoA) results for microbial and virulence

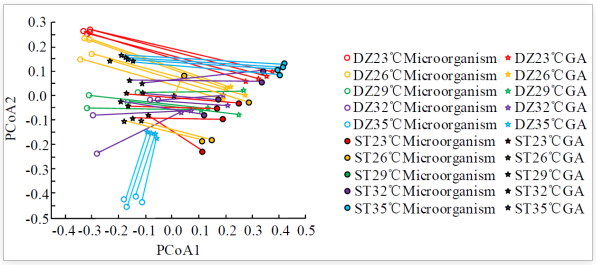

Fig. 7. Procrustes analysis of microbial communities and virulence gene

gene profiles. The x - and y -axes correspond to PCoA 1 and PCoA 2 , respectively, reflecting community composition variation. Microbial communities and GA genes showed strong correlation ($r = 0.810, p < 0.05$), with tightly aligned sample points. This visualized the high degree of structural coupling between the two communities and suggested that the composition pattern of virulence genes was highly dependent on microbial community structure. These findings indicated that microbial communities and virulence genes responded synergistically to environmental disturbances caused by animal carcass decomposition.

3.3. The relationship between environmental factors and metagenomic features

The decomposition of animal carcasses in river water presented a clear coupling disturbance effect between physicochemical parameters and microbial communities. The study found that the decomposition of the corpse led to a decrease in dissolved oxygen (DO) concentration to $0.08mg/L$ and an increase in ammonium nitrogen concentration to 14.32μ g/ml. This extreme condition of hypoxia and nitrogen enrichment was produced under the controlled static water body and fixed corpse load conditions in this study. The degree of dissolved oxygen consumption was higher than reported values in some naturally flowing water bodies, but the accumulation range of ammonium nitrogen was highly similar to the physicochemical characteristics observed by Parida in the polluted section of the Yamuna River, confirming the universality of organic pollution's stress on aquatic ecosystems [15]. Microbial community analysis showed that bacteria remained the dominant group, with relative abundance above 0.6 . However, the abundance of archaea significantly increased in the carcass group ($p < 0.05$). This finding echoed the viewpoint of Pedrinho, who suggested that microbial diversity played a key role in ecosystem resilience-implying that hypoxic stress might have selectively enriched anaerobic archaea, reshaping the community to adapt to envi-

ronmental fluctuations [16]. Notably, the β diversity of microbial communities in the carcass group showed a turning point at 32°C. This observation aligned with the finding by the Cornell research group that the relationship between environmental disturbance intensity and microbial network stability was nonlinear [17]. It suggested that temperature and nutrient loading during decomposition may have interacted to disrupt the stability of microbial communities. In addition, Wang Y and colleagues developed a microbial-induced calcium carbonate precipitation technique, which demonstrated that microbial functional genes could respond to environmental signals by regulating metabolic pathways. This provided mechanistic insight into why virulence genes such as phoP and *g* ln *Al* reached peak abundance at 32°C in this studysuggesting that hypoxic and nitrogen-rich stress might have activated specific regulatory pathways, promoting virulence gene expression and enrichment [18].

The response patterns of virulence genes revealed the potential ecological risks of carcass decomposition. In this study, the carcass group exhibited significantly higher virulence gene abundance compared to the control group. Procrustes analysis further confirmed a strong correlation between virulence gene patterns and microbial community structure ($r = 0.810$), which supported the conclusion by Rasmi et al. that virulence gene distribution was closely linked to microbial ecological niches. Interestingly, the explanatory power of temperature for virulence gene profiles followed a U-shaped trend, reaching a minimum of 0.45 at 26°C and rising to 0.75 at 35°C. This nonlinear pattern resembled the threshold effect reported by Amaral and colleagues, who found that hydrological disturbances influenced the functional structure of river invertebrates [19]. Similarly, when environmental stress surpassed a certain threshold, the enrichment pattern of virulence genes appeared to shift from random diffusion to deterministic selection. From an applied perspective, the deep learning-based real-time monitoring system developed by Mokayed and other researchers, although designed for human health diagnostics, utilized multi-scale feature fusion. This algorithmic logic could be extended to virulence gene risk assessment. By integrating multidimensional data such as DO, $NH_4 - N$, microbial community composition, and virulence gene abundance, predictive models could be constructed for environmental health evaluation [20]. Moreover, the shift toward deterministic environmental filtering at 35°C indicated that high temperatures accelerated the decomposition process, strengthening environmental selection pressure. This, in turn, might have promoted the fixation and transmission of virulence genes within microbial communities.

Yosri et al.'s study emphasized the importance of monitoring fungal communities in assessing the resilience of aquatic environments [21]. Microbial communities are not passively manipulated by the environment. In the early stage of corpse decomposition, the community may buffer environmental changes and maintain basic decomposition and material cycling functions through its inherent functional redundancy, which may correspond to the plateau period of changes in the abundance of certain virulence genes in this study. However, when environmental pressure continues to increase and exceeds a certain ecological threshold, the community structure undergoes a drastic and nonlinear transition, forming a new "disturbance dynamic" steady state that adapts to the stressful environment. The observed turning point of microbial beta diversity around 32°C and the strongest deterministic selection of virulence gene community assembly at 28°C are likely indicative of this steady-state transition critical point. This indicates that the resilience of ecosystems is not infinite, and the impact of highintensity point source pollution may push them towards a functionally distinct new steady state characterized by increased anaerobic metabolism and potential pathogenic risks. Gad et al. directly linked community changes with ecosystem functions by focusing on groups such as protozoa that have clear functional indicators [22]. This provides important methodological insights for this study. When assessing pollution risks, association analysis between specific functional microbial groups (and the functional genes they carry) can more accurately predict ecological health consequences. This study is a deepening of this idea: it not only observed the enrichment of functional groups such as methanogenic archaea and archaea, but also directly captured the expansion and weight of the virulence gene pool that occurred with their enrichment through metagenomics. For example, the enrichment of *g* ln *Al* genes related to nitrogen stress and phoP genes related to global stress response is direct evidence at the molecular level of microbial communities' "metabolic recombination" and "stress preparedness" to adapt to new environments. Therefore, the environmental risk of animal carcass input events lies not only in the instantaneous hypoxia and eutrophication caused by it, but also in the possibility that it may persistently alter the functional gene reserves of water microbial communities, increase the possibility of toxicity factors being stored, transferred, and expressed in the environment, and thus constitute a potential, long-term hotspot for the transmission of zoonotic diseases.

This has important implications for environmental risk

assessment, as traditional assessment methods based on a single physical and chemical indicator may not fully capture ecological risks mediated by microorganisms, such as increased pathogenic potential. The results of this study suggest that a multi-level integrated risk assessment framework should be established: by monitoring changes in key physical and chemical factors, combined with high-throughput sequencing to analyze microbial community structure and the abundance and diversity of functional genes such as virulence genes and antibiotic resistance genes, to comprehensively evaluate the potential threat of organic pollution events to aquatic ecosystem health and public health.

4. Conclusion

The study systematically revealed the multidimensional disturbance effects of animal carcass decomposition on river ecosystems. At the physicochemical level, carcass decomposition significantly reduced DO in the water, with a minimum of 0.08 mg/L, and $NH_4 - N$ concentration, reaching up to 14.32μ g/ml. This created a hypoxic and high-nitrogen stress environment, consistent with the process of oxygen consumption and nitrogenous organic matter release during decomposition. At the microbial community level, bacteria remained the dominant group, but the abundance of archaea significantly increased in the carcass group ($p < 0.05$). The β diversity of communities showed a "decrease-then-increase" trend with rising temperature, and at 35°C, stochastic community assembly shifted toward deterministic environmental selection. At the virulence gene level, virulence genes such as phoP and g ln Al had significantly higher abundance in the carcass group compared to the control group, peaking at 32°C. Procrustes analysis confirmed a strong coordination between virulence gene profiles and microbial communities (r = 0.810). The results demonstrated that animal carcass decomposition in river water altered the microenvironment, driving microbial community restructuring and promoting virulence gene enrichment and cooccurrence, thereby increasing the pathogenic risk to the aquatic ecosystem. These findings not only clarify the hierarchical mechanism of animal carcass decomposition driving the enrichment of virulence genes, namely environmental stress → community screening → functional response, but more importantly, they collectively constitute a conceptual framework for the integrated assessment of key environmental factors, microbial community dynamics, and virulence gene risks, providing new theoretical basis for early warning and assessment of health risks of organic pollution in rivers from the dimension of 'microbial function'. However, natural river water is dynamic,
and the study's experimental design did not account for water flow effects on microbial communities. Future work will further optimize the simulation of water circulation by employing inflow-outflow experimental setups to better investigate the complex multilevel effects of carcass decomposition in flowing water environments. In addition, factors such as hydrodynamic conditions (such as flow velocity, turbulence), interactions at the water sediment interface, seasonal climate changes (such as temperature, rainfall fluctuations), and different types and quantities of animal carcasses may also have significant impacts on decomposition processes, microbial community succession, and the spread of virulence genes. Incorporating these factors into future research frameworks will help build more comprehensive and realistic risk assessment models for river ecosystems.

References

[1] A. Talema, (2023) *"Causes, negative effects, and preventive methods of water pollution in Ethiopia"* **Quality Assurance and Safety of Crops & Foods** ***15***(2): 129–139. DOI: 10.15586/qas.v15i2.1271.

[2] M. L. Viljur, S. R. Abella, and M. Adámek, (2022) *"The effect of natural disturbances on forest biodiversity: an ecological synthesis"* **Biological Reviews** ***97***(5): 1930–1947. DOI: 10.1111/brv.12876.

[3] C. Yang, Z. Zeng, Y. Wang, G. He, and Y. Hu, (2023) *"Ecological risk assessment and identification of the distinct microbial groups in heavy metal-polluted river sediments"* **Environmental Geochemistry and Health** ***45***(5): 1311–1329. DOI: 10.1007/s10653-022-01343-4.

[4] G. Barceló, P. L. Perrig, P. Dharampal, E. Donadio, and S. A. Steffan, (2022) *"More than just meat: carcass decomposition shapes trophic identities in a terrestrial vertebrate"* **Functional Ecology** ***36***(6): 1473–1482. DOI: 10.1111/1365-2435.14041.

[5] A. H. Rasmi, E. F. Ahmed, A. M. A. Darwish, and G. F. M. Gad, (2022) *"Virulence genes distributed among Staphylococcus aureus causing wound infections and their correlation to antibiotic resistance"* **BMC Infectious Diseases** **22**(1): 652–663. DOI: 10.1186/s12879-022-07624-8.

[6] I. K. Hamasalih, A. M. Salih, S. J. M. Sdiq, K. Q. Yaqub, and S. M. Raheem, (2025) *"Tanjaro River pollution and its impact on the aquatic food chain"* **Science and Education** ***5***(3): 235–244. DOI: 10.55677/ijssers/V05I03Y2025-01.

[7] D. Onyejike, U. G. Esomonu, V. A. Fischer, I. M. Onyejike, and E. N. Ezenwatu, (2022) *"Visible post mortem changes as a tool for decomposition timeline estimation in a tropical rainforest vegetation of Nigeria"* **Tropical Journal of Medical Research *21***(1): 49–60. DOI: 10.5281/zenodo.6568722.

[8] A. Khalil, M. M. M. Zidan, R. Alajmi, and A. M. Ahmed, (2023) *"Impact of envenomation with snake venoms on rabbit carcass decomposition and differential adult dipteran succession patterns"* **Journal of Medical Entomology *60***(1): 40–50. DOI: 10.1093/jme/tjac173.

[9] M. Daniels, S. Reynolds, and D. Umstead, (2025) *"Assessment of common nutrient levels and water quality in town run tributary of the Potomac river"* **Proceedings of the West Virginia Academy of Science *97***(2): 19–32. DOI: 10.55632/pwvas.v97i2.1187.

[10] S. M. Syed Mohd Daud, C. C. Heo, M. Y. P. Mohd Yusof, L. S. Khoo, and M. K. Chainchel Singh, (2024) *"Use of thermal drone in detection and assessment of larval mass temperature in decomposed rabbit carcasses"* **Journal of Forensic Sciences *69***(2): 542–553. DOI: 10.1111/1556-4029.15466.

[11] E. Wenting, P. A. Jansen, S. Burggraeve, D. F. Delsman, and H. L. Siepel, (2024) *"The influence of vertebrate scavengers on leakage of nutrients from carcasses"* **Oecologia *206***(1): 21–35. DOI: 10.1007/s00442-024-05608-w.

[12] P. Borah, R. Dutta, L. Das, G. Hazarika, and M. Choudhury, (2022) *"Prevalence, antimicrobial resistance and virulence genes of Salmonella serovars isolated from humans and animals"* **Veterinary Research Communications *46***(3): 799–810. DOI: 10.1007/s11259-022-09900-z.

[13] M. Ahmadi, R. Ranjbar, P. Behzadi, and T. Mohammadian, (2022) *"Virulence factors, antibiotic resistance patterns, and molecular types of clinical isolates of Klebsiella Pneumoniae"* **Expert Review of Anti-Infective Therapy *20***(3): 463–472. DOI: 10.1080/14787210.2022.1990040.

[14] Z. Bourhane, A. Lanzén, C. Cagnon, O. B. Said, and E. Mahmoudi, (2022) *"Microbial diversity alteration reveals biomarkers of contamination in soil-river-lake continuum"* **Journal of Hazardous Materials *421***: 126789. DOI: 10.1016/j.jhazmat.2021.126789.

[15] P. K. Parida, B. K. Behera, B. Dehury, A. K. Rout, and D. J. Sarkar, (2022) *"Community structure and function of microbiomes in polluted stretches of river Yamuna in New Delhi, India, using shotgun metagenomics"* **Environmental Science and Pollution Research *29***(47): 71311–71325. DOI: 10.1007/s11356-022-20766-1.

[16] A. Pedrinho, L. W. Mendes, A. P. de Araujo Pereira, A. S. F. Araujo, and A. Vaishnav, (2024) *"Soil microbial diversity plays an important role in resisting and restoring degraded ecosystems"* **Plant and Soil *500***(1): 325–349. DOI: 10.1007/s11104-024-06489-x.

[17] C. R. Cornell, Y. Zhang, and D. Ning, (2023) *"Land use conversion increases network complexity and stability of soil microbial communities in a temperate grassland"* **The ISME Journal *17***(12): 2210–2220. DOI: 10.1038/s41396-023-01521-x.

[18] Y. Wang, G. Wang, Y. Wan, X. Yu, and J. Zhao, (2022) *"Recycling of dredged river silt reinforced by an eco-friendly technology as microbial induced calcium carbonate precipitation (MICP)"* **Soils and Foundations *62***(6): 101216. DOI: 10.1016/j.sandf.2022.101216.

[19] D. P. H. M. Amaral, D. M. P. de Castro, M. S. Linares, R. M. Hughes, and E. van den Berg, (2025) *"Small hydropower dam alters the functional structure of macroinvertebrate assemblages in a Neotropical savanna river"* **Hydrobiologia *852***(12): 3137–3154. DOI: 10.1007/s10750-024-05720-1.

[20] H. Mokayed, T. Z. Quan, L. Alkhaled, and V. Sivakumar, (2023) *"Real-time human detection and counting system using deep learning computer vision techniques"* **Artificial Intelligence and Applications *1***(4): 221–229. DOI: 10.47852/bonviewAIA2202391.

[21] M. Yosri, A. Z. A. Herrawy, S. M. Bassem, E. E. Hafez, A. M. Abu-Elsaoud, and M. I. Abo-Alkasem, (2025) *"Aquatic environments resilience: Third-generation sequencing of fungi community of urban wastewater treatment plant and Nile River (Egypt)"* **Euro-Mediterranean Journal for Environmental Integration *10***(1): 15–23. DOI: 10.1007/s41207-024-00600-5.

[22] M. Gad, M. Yosri, M. E. Fawzy, A. K. Saleh, H. M. R. Abdel-Latif, A. M. Abu-Elsaoud, M. M. El-Sheekh, and M. I. Abo-Alkasem, (2024) *"Microeukaryotic communities diversity with a special emphasis on protozoa taxa in an integrated wastewater treatment system"* **Environmental Sciences Europe *36***(1): 101. DOI: 10.1186/s12302-024-00907-8.